JOURNAL OF VIROLOGY, June 2001, p. 5375–5380 Vol. 75, No. 11
0022-538X/01/$04.00+0 DOI: 10.1128/JVI.75.11.5375–5380.2001

Structural Analysis of a Fiber-Pseudotyped Adenovirus with Ocular Tropism Suggests Differential Modes of Cell Receptor Interactions

CHARLES Y. CHIU,[1] EUGENE WU,[2] SWATI L. BROWN,[2] DAN J. VON SEGGERN,[2] GLEN R. NEMEROW,[2]* AND PHOEBE L. STEWART[1]*

Department of Molecular and Medical Pharmacology and Crump Institute for Molecular Imaging, UCLA School of Medicine, Los Angeles, California 90095,[1] and Department of Immunology, The Scripps Research Institute, La Jolla, California 92037[2]

Received 1 November 2000/Accepted 26 February 2001

Adenovirus (Ad) entry into cells is initiated by the binding of the fiber knob to a cell surface receptor. The coxsackie- and adenovirus receptor (CAR) functions as the attachment receptor for many, but not all, Ad serotypes. Ad type 37 (Ad37), a subgroup D virus that causes keratoconjunctivitis in humans, does not infect cells via CAR despite demonstrated binding of the Ad37 knob to CAR. We have pseudotyped a fiber deletion Ad5 vector with the Ad37 fiber (Ad37f), and this vector retains the ocular tropism of Ad37. Here we present a cryo-electron microscopy reconstruction of Ad37f that shows the entire Ad37 fiber, including the shaft and knob domains. We have previously proposed that Ad37 may not utilize CAR for cell entry because of the geometric constraints imposed by a rigid fiber (E. Wu, J. Fernandez, S. K. Fleck, D. Von Seggern, S. Huang, and G. R. Nemerow, Virology 279:78–89, 2001). Consistent with this hypothesis, our structural results show that the Ad37 fiber is straight and rigid. Modeling of the interaction between Ad37f and host cell receptors indicates that fiber flexibility or rigidity, as well as length, can affect receptor usage and cellular tropism.

Viral cell entry is a complex process that is initiated by the specific interaction of capsid proteins with cell surface receptors. Efficient infection of cells by adenovirus (Ad) involves binding to two different receptors (14). The Ad fiber protein recognizes the primary receptor, allowing high-affinity binding of virus particles to the cell surface (10, 15), and an Arg-Gly-Asp (RGD) sequence motif in the Ad penton base promotes association with secondary receptors, $\alpha_v\beta_3$ or $\alpha_v\beta_5$ integrin, triggering virus internalization (32). The coxsackievirus and Ad receptor (CAR) protein was initially identified as the fiber receptor for Ad2 and Ad5 (5, 26) and functions as a receptor for many, but not all, Ad serotypes (17). There are 51 Ad serotypes classified into subgroups A to F, encompassing a broad spectrum of tissue tropisms and disease. Members of Ad subgroups B, C, and E, including Ad type 2 (Ad2) and Ad5, cause respiratory infections; those of subgroups A and F, including Ad12 and Ad40/41, are responsible for gastrointestinal infections; and those of subgroup D, including Ad37, Ad8, and Ad19a, are associated with epidemic keratoconjunctivitis, a highly contagious ocular infection with the potential to impair visual function (4, 9, 16). Understanding the molecular and cellular basis for these differences would assist in the development of novel antiviral drugs as well as improved gene delivery vectors.

The Ad fiber protein is a homotrimeric molecule extending from each of the 12 vertices of the icosahedral capsid. The fiber consists of an N-terminal tail domain that interacts with the Ad penton base, a central shaft domain of variable length, and a C-terminal knob domain that contains the receptor binding site. Sequence analysis indicates that the fiber shaft is composed of 6 to 23 β-repeats in various Ad serotypes (8). The Ad37 fiber has only eight β-repeats (4), making it relatively short. Interestingly, most Ad fibers are not perfectly rigid but exhibit a bent or kinked conformation as viewed by negative-stain electron microscopy (EM) (8). A cryo-EM reconstruction of Ad2 also indicates that the fiber is bent (22). The central shaft domain of most but not all Ad fibers contains a nonconsensus β-repeat element that may confer flexibility to the fiber (8). Notably, the fiber shafts of Ad9, Ad37, and other subgroup D viruses do not have this nonconsensus β-repeat.

Several crystal structures of the fiber knobs from various serotypes have been published (6, 28, 34), including a structure of the Ad12 knob complexed with the N-terminal domain of CAR (6). The structure of the complex reveals that all of the residues involved in binding to CAR are located on the side of the knob and that the majority of the contact residues are in the AB loop. The importance of the AB loop in CAR binding is highlighted by both the conservation of amino acids comprising this loop in CAR binding serotypes and the wide divergence of the AB loop sequences among non-CAR binding serotypes.

The Ad37 fiber knob contains a CAR binding consensus sequence in its AB loop (13), and direct binding of the recombinant Ad37 fiber knob to CAR has been demonstrated (33). Curiously, this serotype does not effectively use CAR as its attachment receptor, as shown by virus binding and infection studies with conjunctival, corneal, and lung epithelial cells (2, 11, 33). It has been suggested that sialic acid (2, 3) or an

* Corresponding author. Mailing address for Phoebe L. Stewart: Department of Molecular and Medical Pharmacology, UCLA School of Medicine, A-324 CIMI, Box 951770, Los Angeles, CA 90095-1770. Phone: (310) 206-7055. Fax: (310) 206-8975. E-mail: pstewart@mednet.ucla.edu. Mailing address for Glen R. Nemerow: Department of Immunology, The Scripps Research Institute, La Jolla, CA 92037. Phone: (858) 784-8072. Fax: (858) 784-8472. E-mail: gnemerow@scripps.edu.

as-yet-unidentified 50-kDa glycoprotein (33) may serve as the attachment receptor for Ad37. Specific ocular cell binding is likely mediated by the 50-kDa protein rather than by sialic acid (33).

Huang et al. (11) have noted that a single lysine residue at position 240 of the Ad37 fiber is critical for binding and infection of conjunctival cells. Molecular modeling of the Ad37 fiber knob based on the Ad5 fiber knob crystal structure (34) indicates that residue 240 is exposed on the top surface of the knob, in the CD loop (11). The CD loop does not contact CAR in the crystal structure of the Ad12 fiber knob-CAR complex (6). Thus, for Ad37, binding via the CD loop most likely involves a receptor other than CAR. Wu et al. (33) have proposed that if Ad37 has a rigid fiber, it might not be able to utilize CAR for cell entry because of geometric constraints. Specifically, a rigid fiber would make it impossible for the virus to present the side of the knob, with the CAR binding AB loop, to CAR on the host cell surface.

Using fiber-pseudotyping technology (21, 31), we produced an Ad5 vector containing the Ad37 fiber (Ad37f) and confirmed that the chimeric virus exhibits ocular cell tropism (33). Cryo-EM combined with single-particle image reconstruction methods has proven useful for analyzing the structure of Ad (22, 24, 25). Here we present a cryo-EM structural study of the pseudotyped Ad37f virus. Modeling of the Ad37f structure with host cell receptors provides additional insight into why CAR is not utilized by Ad37.

Cryo-EM. Cryo-EM images of pseudotyped Ad37f produced from two plasmids, pDV80 and pDV121, were collected (33). The particles produced with pDV80 contained two serendipitous mutations (S356→P and I362→T) in the C terminus of the Ad37 fiber protein. These mutations did not affect trimerization, incorporation into Ad particles, or receptor binding properties. The figures presented in this paper were generated from particles with the fiber mutations. We have also produced particles with the authentic wild-type Ad37 fiber (made with pDV121), and subsequent cryo-EM analysis confirmed that there is no discernible structural difference between the mutated and wild-type fibers.

Purified viral preparations of Ad37f particles were concentrated to ~200 μg/ml, and cryo-plunging was performed as described previously (1, 7). The cryo-grids were examined in a Philips CM120 transmission electron microscope equipped with a LaB_6 filament, a Gatan cryo-transfer holder, and a Gatan slow-scan CCD camera (1,024 by 1,024 pixels). Digital images were collected under low-dose conditions ($<20\ e^-/Å^2$) at a nominal magnification of ×45,000 and at three different defocus values (−0.5, −1.0, and −1.5 μm). The digital micrographs had a pixel size of 4.1 Å on the molecular scale.

Image processing. Computer image processing was carried out on Compaq/DEC Alpha workstations (Compaq, Inc.). Individual particle images (387 total) were extracted as 300- by 300-pixel fields by using the QVIEW particle selection program (19). The IMAGIC software package was used for all subsequent image processing and reconstruction steps (27). The Euler orientations within the icosahedral asymmetric triangle were computationally determined, and the three defocus sets were then combined after two-dimensional correction for the contrast transfer function (7). The parameters of the modeled contrast transfer function equation (spherical aberration constant [Cs] = 2 mm, fraction of amplitude contrast = 0.1, kilovolts = 120, decay constant = 10 nm^2, Fermi filter resolution cutoff = 8.1 Å, filter width = 3 Å, and defocus = −0.5, −1.0, or −1.5 μm) were chosen to minimize "ringing" in the particle images. Three-dimensional reconstruction of the Ad37f particle was carried out by the exact filter back-projection technique after two cycles of anchor set refinement (7). The resolution of the Ad37f reconstruction was assessed using the Fourier shell correlation 0.5 threshold criterion after applying "soft" masks to each half-reconstruction (23). The calculated resolution of the reconstruction is 24 Å. Isosurface representations of the reconstruction were displayed using AVS graphical software (Advanced Visualization Systems, Inc.). The Ad37f reconstruction was contoured to correspond to a continuous, "nonholey" viral capsid. The density of the fiber was noted to be ~50% of that of the viral capsid, and thus the fiber is contoured with a lower isosurface value. The lower fiber density may be attributed to partial occupancy of the fiber in the pseudotyped Ad37f particles.

Several attempts were made to calculate a reconstruction of the Ad37f structure without imposing full icosahedral (532) symmetry in order to visualize the fiber density without imposed fivefold symmetry. First, we tried to determine the correct Euler orientations for the 387 particle images assuming either no symmetry or D3 (32) symmetry. In a separate approach, we generated an anchor set of reprojections of the icosahedral Ad37f reconstruction evenly spanning the D3 asymmetric unit and used these reprojections to search for D3 Euler angles for the particle images. Unfortunately, none of these methods yielded reasonable three-dimensional reconstructions. However, our interpretation of the interaction of Ad37 with host cell receptors relies mainly on structural features (length and rigidity) that are not affected by the fivefold symmetrization of the fiber density.

Features of the Ad37f reconstruction. The cryo-EM reconstruction of Ad37f is presented in Fig. 1 and compared to two clear cryo-EM particle images that show density corresponding to the knobs at the ends of the short Ad37 fibers. In a cryo-EM particle image, all of the viral density is projected into the two-dimensional image plane; thus, fibers that are not overlapping with the capsid or obscured by the carbon support film or background noise can be observed. Surface views of the three-dimensional reconstruction were generated to match the orientations of these two particle images. The comparison between Fig. 1A and B indicates that the two regions of strongest knob density correspond to superimposed fiber knobs. The particle image in Fig. 1C is oriented close to a fivefold-symmetry axis, and at least five fibers are visible. The positions of these fibers correspond well with 5 of the 10 fibers that are observed to project radially around the reconstruction in this view (Fig. 1D). The fact that the reconstructed fiber knobs are found in the same positions as the knobs visible in the particle images suggests that the Ad37 fiber is properly reconstructed and that the Ad37 fiber is rigid and straight.

The dimensions of the Ad37 knob observed in the Ad37f reconstruction (70 by 80 by 80 Å) agree well with those expected from the crystal structures of knobs from other Ad serotypes (6, 28, 34). A top view of the reconstructed vertex region shows the fiber knob having a fivefold-symmetric appearance, when in reality it is trimeric (Fig. 2A). The Ad37

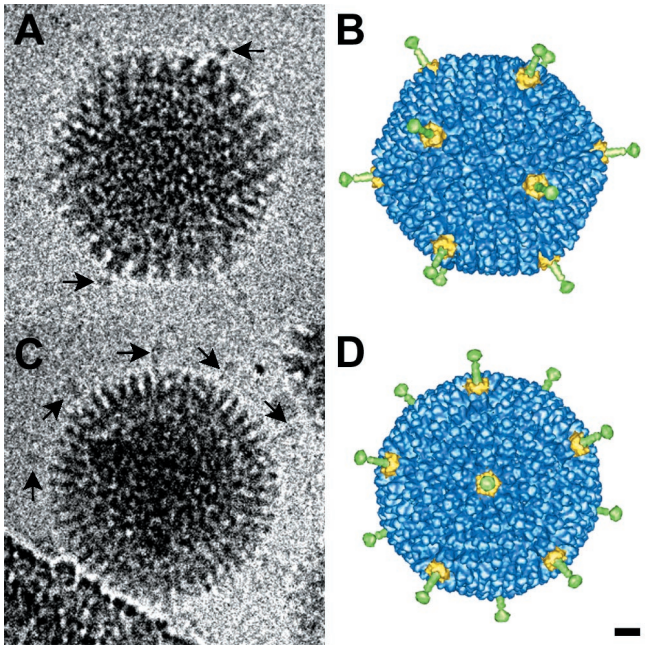

FIG. 1. Cryo-EM particle images and reconstruction of the Ad37f pseudotyped vector. (A and C) Two clear particle images showing density around the capsid corresponding to the short fibers. (B and D) Surface views of the three-dimensional reconstruction shown in the same orientations as determined for the particle images in panels A and C. The arrows in panel A point to strong density from overlapping fiber knobs. The arrows in panel C point to five fibers visible around the capsid in this approximate fivefold view. The fiber is colored green, the penton base is yellow, and the remaining capsid is blue. Bar, 100 Å.

fiber protein, including the knob, is observed to extend approximately 150 Å from the surface of the capsid (Fig. 2B). In contrast, previous cryo-EM studies of Ad2, Ad5, and Ad12 revealed long fibers (>300 Å) in the particle images, yet only 60 to 100 Å of the shaft was reconstructed with strong density (7, 24, 31). After this point, the Ad2 fiber density becomes weaker and spreads out in a cone-like distribution (Fig. 2C). This indicates a bend or kink in the fiber shaft at roughly the same location noted by negative-stain EM (8). The observations that the Ad2 fiber density tapers off significantly while the Ad37 fiber density is equally strong throughout its length support our conclusions that the Ad2 fiber is bent and likely flexible, while the Ad37 fiber is straight and rigid.

Modeling with the fiber knob crystal structure. The crystal structure of the Ad2 fiber knob and a portion of the shaft (28) was manually positioned within the reconstructed cryo-EM Ad37f fiber density. The amino acid sequence of the Ad37 knob domain is 46% identical and 60% similar to that of the Ad2 knob domain, and hence modeling with the Ad2 crystal structure is reasonable. The fit along the fiber axis was clear, with very little ambiguity in the height (Fig. 3A). For the rotational fit, we positioned the prominent HI loop into a density bulge on the side of the knob, considering only one-fifth of the reconstructed knob density (Fig. 3B). As discussed previously, there is a symmetry mismatch between the icosahedral reconstruction and the trimeric fiber. Note that the AB loop, involved in CAR binding, is on the side of the knob, while the CD loop, involved in binding to the 50-kDa receptor, is located more towards the top of the knob. These findings are consistent with the idea that for Ads with short rigid fibers, only the top, rather than the side, of the knob is available for receptor binding (33).

Ad37 uses α_v integrins as coreceptors. One consequence of the short, inflexible Ad37 fiber is that there is a different spatial relationship between the fiber knob and penton base receptor binding sites than found for serotypes such as Ad2 and Ad5, with long, flexible fibers. Thus, we wondered what effect the Ad37 geometry would have on coreceptor binding. Previous studies had indicated that wild-type Ad37 virus particles are capable of efficient binding to soluble recombinant integrin $\alpha_v\beta_5$ (12). The amino acid sequence of the Ad37 penton base indicates that it contains the conserved RGD integrin binding motif (3). To confirm that the Ad37f pseudotyped vector uses α_v integrins for infection, we performed competition studies using the green fluorescent protein (GFP) reporter assay.

Adherent Chang C human conjunctival cells were incubated with 100 μg of HB5 (anti-CD21) antibody, LM609 (anti-$\alpha_v\beta_3$)

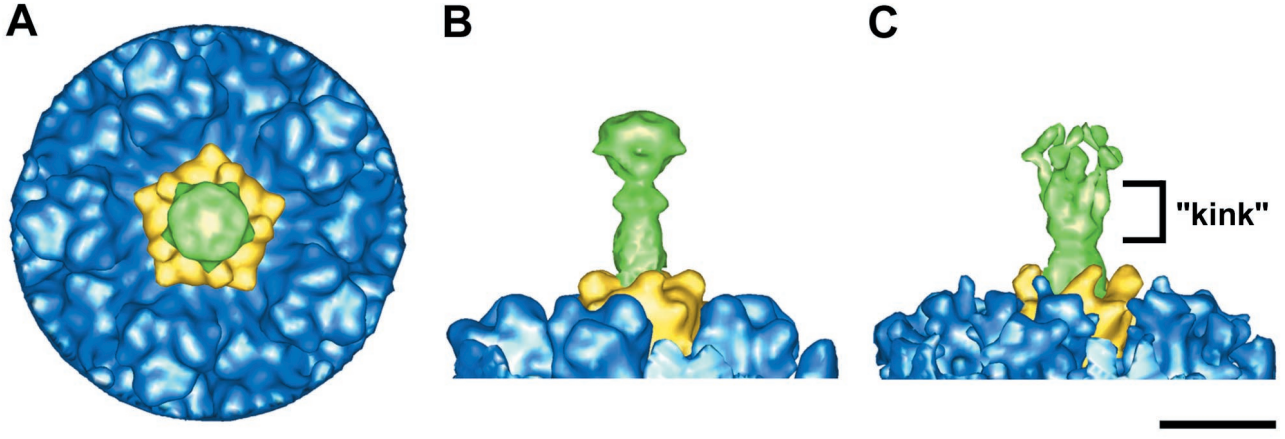

FIG. 2. Vertex region of the Ad37f pseudotyped vector and comparison with Ad2. (A and B) Top and side views of the Ad37f vertex region. (C) Side view of the Ad2 vertex region (7) shown with a low isosurface value to include the weak diffuse density that results from flexibility in the fiber shaft. The color scheme is the same as in Fig. 1. Bar, 100 Å.

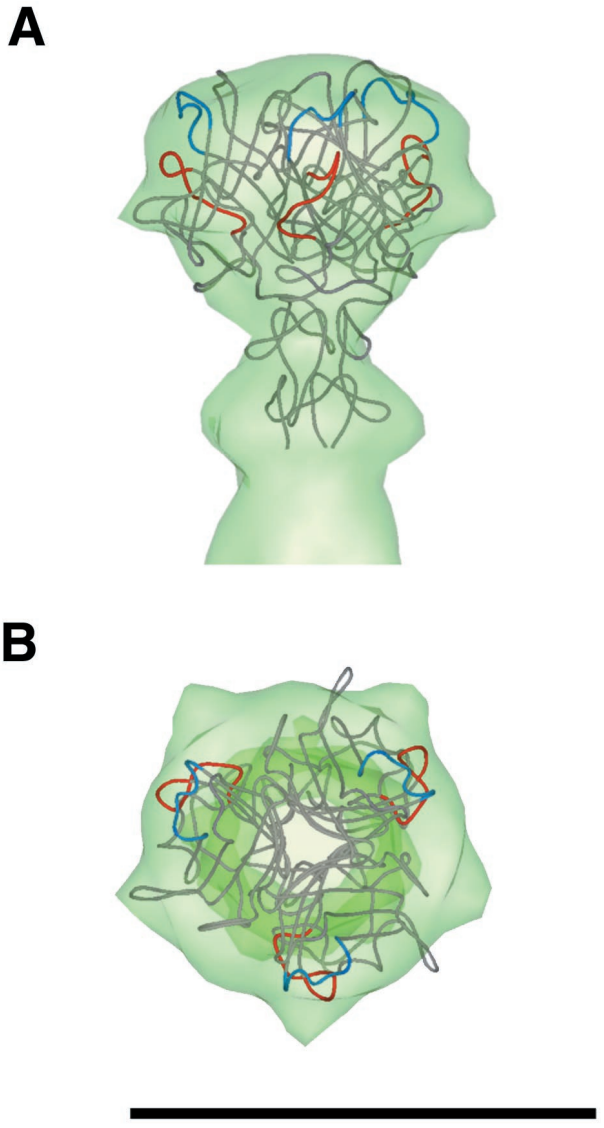

FIG. 3. Modeling of the crystal structure of the Ad2 knob and a portion of the shaft into the Ad37f cryo-EM fiber density. (A) Side view. (B) Top view. The AB loop is colored red, and the CD loop is blue. The arrows point to the HI loop that protrudes in the Ad2 crystal structure (29) and fits well within a bulge of the reconstructed Ad37f fiber knob. Bar, 100 Å.

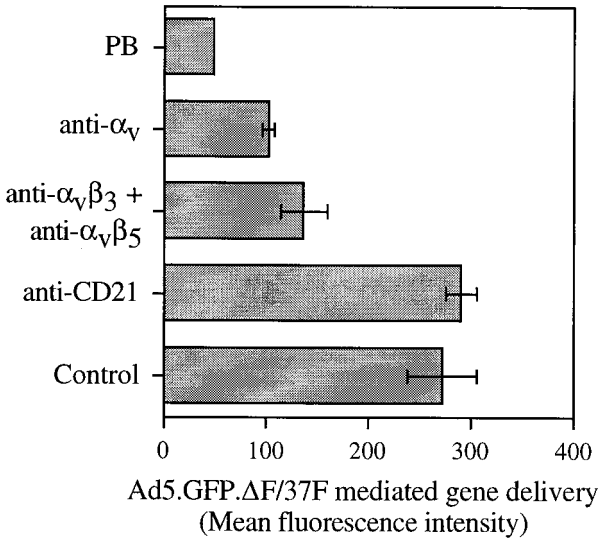

FIG. 4. Pseudotyped Ad with Ad37 fiber uses α_v integrins for internalization. Chang C cells were pretreated with 100 μg of HB5 (anti-CD21) monoclonal antibody, LM609 (anti-$\alpha_v\beta_3$) and P1F6 (anti-$\alpha_v\beta_5$) monoclonal antibodies, 69-6-5 (anti-α_v) antibody, or recombinant Ad5 penton base (PB) per ml in Dulbecco's modified Eagle medium with 10% fetal bovine serum for 1 h at 37°C before infection with Ad5.GFP.ΔF/37F. Cell fluorescence from GFP transgene expression was measured by flow cytometry. Error bars indicate standard deviations from three experiments. The error for the penton base experiment was too small to show on the graph.

and P1F6 (anti-$\alpha_v\beta_5$) antibodies, 69-6-5 (anti-α_v) antibody, or recombinant Ad5 penton base per ml (32) in Dulbecco's modified Eagle medium with 10% fetal bovine serum for 1 h at 37°C. Ad5.GFP.ΔF/37F was then added at 10,000 particles per cell and incubated for 3 h at 37°C. The cells were then washed twice and cultured overnight. Eighteen to 20 h later, cells were detached with buffer containing 0.05% (wt/vol) trypsin and 0.5 mM EDTA (Boehringer Mannheim) for 5 min at 37°C and washed with phosphate-buffered saline, pH 7.4. GFP fluorescence was measured with a FACScan flow cytometer. A threshold established by the fluorescence of uninfected cells was used to distinguish cells specifically expressing GFP. As shown in Fig. 4, pretreatment of cells with soluble penton base or with function-blocking monoclonal antibodies to α_v or $\alpha_v\beta_3$ and $\alpha_v\beta_5$ integrins significantly reduced Ad37f-mediated gene delivery. Pretreatment of cells with a CD21-specific (control) antibody had no effect. These studies indicate that the pseudotyped virus recognizes α_v integrins and is capable of using these coreceptors for infection.

We then attempted to model the $\alpha_v\beta_5$ integrin cryo-EM density over the penton base of the Ad37f reconstruction. In the absence of a crystal structure for $\alpha_v\beta_5$ integrin, we used the cryo-EM density observed in the Ad12-$\alpha_v\beta_5$ complex for structural modeling (7). In Fig. 5, we show the integrin density positioned over the vertex region of the Ad37f reconstruction. The height of the integrin density is known to vary with the length of the RGD loop of the penton base (7). In the pseudotyped Ad37f vector, the penton base is that of Ad5, and the length of the RGD loop of Ad5 (80 residues) is almost identical to that of Ad2 (82 residues). Thus, we based the height of the integrin density over the Ad5 penton base on the observed height in the published Ad2-$\alpha_v\beta_5$ complex reconstruction (7). We chose to use the integrin density from the Ad12 complex, rather than that from the Ad2 complex, since the longer and more flexible Ad2 RGD loops resulted in weak and diffuse reconstructed integrin density (7). The integrin density shown corresponds to the extracellular portion of $\alpha_v\beta_5$, and the position of the host cell membrane is presumed to be directly above it in vivo.

The model indicates that the height of the extracellular $\alpha_v\beta_5$ integrin density is roughly equivalent to that of the Ad37 fiber. Concurrent binding of the knob with a cell receptor and penton base with integrin could occur if the Ad37 fiber receptor contains a relatively small ectodomain and/or this domain lies

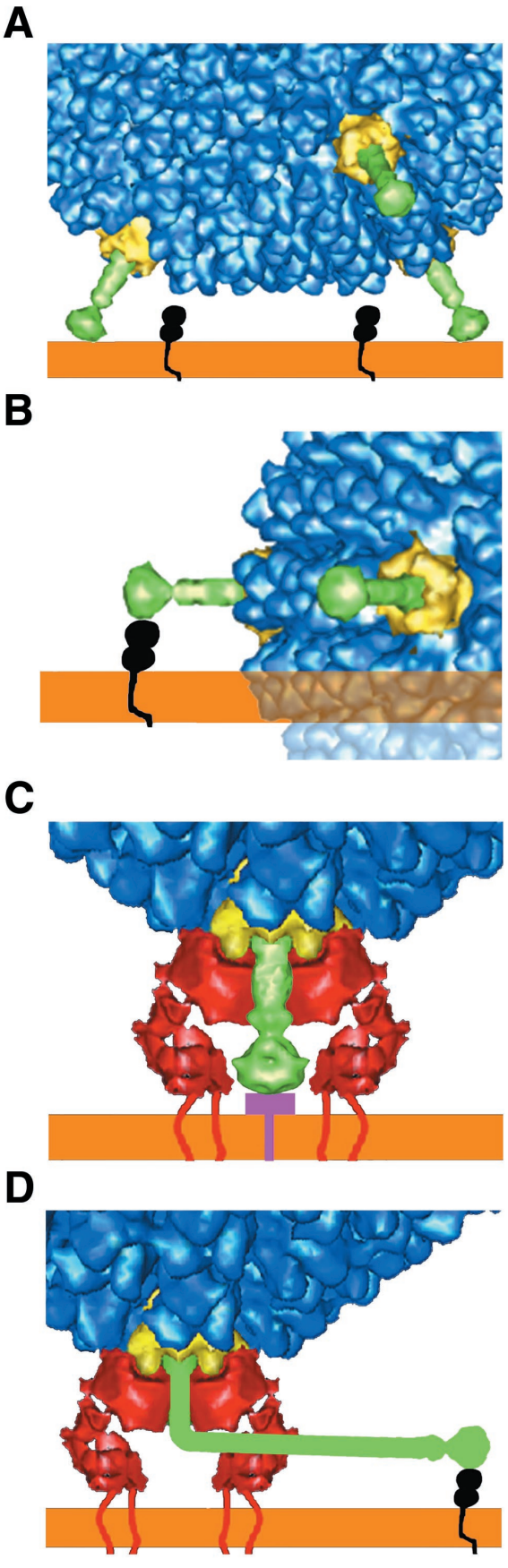

nearly flat against the cell surface. For CAR binding Ad serotypes with long, flexible fibers, concurrent binding of penton base with α_v integrin at the same vertex is feasible if a maximum of four integrin binding sites are occupied on the penton base, thus leaving room for the bent fiber shaft (Fig. 5).

Implications for other Ad serotypes. Shayakhmetov and Lieber (20) showed that modified Ad5 particles containing the short Ad9 fiber shaft have reduced CAR binding and infection. Experiments were carried out using Ad5 vectors with one of two different CAR binding fiber knobs, Ad5 or Ad9, together with either the long shaft of Ad5 or the short shaft of Ad9 (20). Our cryo-EM studies of Ad5 (30) indicate that the Ad5 fiber shaft is bent. We presume from published sequence data that the short Ad9 fiber shaft is rigid, since it does not have the nonconsensus β-repeat motif found in flexible Ad fibers (8). This presumption is corroborated by the fact that the Ad37 fiber shaft is also missing the nonconsensus β-repeat, and the results presented here show that the Ad37 fiber is straight. These observations add a new twist to the study by Shayakhmetov and Lieber in that not only were the lengths of the shafts different but also one shaft was bent while the other most likely was straight. They found that for Ad5 vectors with either CAR binding knob, a long fiber shaft was important for efficient adsorption and transduction of CAR-α_v integrin-expressing cells. In light of the cryo-EM studies, fiber shaft flexibility, as well as length, plays a role in receptor usage.

It is likely that all of the fiber proteins of subgroup B Ads, which lack CAR binding activity, have straight, rigid structures. In support of this, a cryo-EM reconstruction of the Ad3 penton base-fiber dodecahedron shows that the fiber is rigid and even shorter than those of Ad37 and Ad9 (18). It is known that Ad3 does not bind to CAR and does not contain the CAR binding consensus sequence (6). From our results, we predict that Ad3, like Ad37, uses a non-CAR fiber receptor that binds to the top surface of the knob.

Others have shown that Ad serotypes with fiber knobs containing a consensus CAR binding sequence do not necessarily bind CAR on cells (2). Our results indicate that the flexibility or rigidity of the Ad fiber plays a role in determining which fiber receptors can be utilized for cell entry. These structural and modeling studies show that the geometrical constraints imposed by a short rigid fiber protruding from an icosahedral viral capsid effectively prevent use of the side of the fiber knob for receptor binding. Thus, fiber flexibility, as well as length, appears to play a heretofore unappreciated role in receptor selectivity and in viral tropism. The knowledge gained from these studies improves our understanding of the structural

FIG. 5. Interaction of Ad37 and Ad2 with their cell receptors. (A) The geometry of Ad37 with short, rigid fibers (green) prevents the side of the fiber knob from contacting the appropriate surface of CAR (black). (B) If the side of the fiber knob on Ad37 were to bind CAR, there would be steric hindrance between the viral capsid and the host cell membrane (orange). The clash is indicated by transparent density. (C) Ad37 is shown binding a 50-kDa receptor that is preferentially expressed on conjunctival cells (33). Modeling indicates that concurrent binding of the fiber with the 50-kDa receptor (purple) and of the penton base (yellow) with α_v integrin (red) should be possible. (D) The Ad types with long, bent fibers, such as Ad2 and Ad5, contact CAR with the side of the fiber knob.

basis of Ad-receptor interactions and may serve as a guide for retargeting of Ad vectors to specific cell types in vivo.

We thank Shuang Huang for helpful advice on Ad37 receptor interactions.

This work was supported by grants from the National Institutes of Health (AI42929 to Phoebe L. Stewart and HL54352 and EY11431 to Glen R. Nemerow) and by Genetic Therapy Inc./Novartis grant SFP1089. Charles Chiu was supported by an NIH-MSTP training grant (GM08042) and the Aesculapians fund of the UCLA School of Medicine.

REFERENCES

1. **Adrian, M., J. Dubochet, J. Lepault, and A. W. McDowall.** 1984. Cryo-electron microscopy of viruses. Nature **308:**32–36.
2. **Arnberg, N., K. Edlund, A. H. Kidd, and G. Wadell.** 2000. Adenovirus type 37 uses sialic acid as a cellular receptor. J. Virol. **74:**42–48.
3. **Arnberg, N., A. H. Kidd, K. Edlund, F. Olfat, and G. Wadell.** 2000. Initial interactions of subgenus D adenoviruses with A549 cellular receptors: sialic acid versus alpha(v) integrins. J. Virol. **74:**7691–7693.
4. **Arnberg, N., Y. Mei, and G. Wadell.** 1997. Fiber genes of adenoviruses with tropism for the eye and the genital tract. Virology **227:**239–244.
5. **Bergelson, J. M., J. A. Cunningham, G. Droguett, E. A. Kurt-Jones, A. Krithivas, J. S. Hong, M. S. Horwitz, R. L. Crowell, and R. W. Finberg.** 1997. Isolation of a common receptor for coxsackie B viruses and adenoviruses 2 and 5. Science **275:**1320–1323.
6. **Bewley, C. M., K. Springer, Y. B. Zhang, P. Freimuth, and J. M. Flanagan.** 1999. Structural analysis of the mechanism of adenovirus binding to its human cellular receptor, CAR. Science **286:**1579–1583.
7. **Chiu, C. Y., P. Mathias, G. R. Nemerow, and P. L. Stewart.** 1999. Structure of adenovirus complexed with its internalization receptor, αvβ5 integrin. J. Virol. **73:**6759–6768.
8. **Chroboczek, J., R. W. H. Ruigrok, and S. Cusack.** 1995. Adenovirus fiber, p. 163–200. *In* W. Doerfler and P. Böhm (ed.), The molecular repertoire of adenoviruses, vol. 199, part I. Springer-Verlag, New York, N.Y.
9. **Curtis, S., G. W. Wilkinson, and D. Westmoreland.** 1998. An outbreak of epidemic keratoconjunctivitis caused by adenovirus type 37. J. Med. Microbiol. **47:**91–94.
10. **Defer, C., M. T. Belin, M. L. Caillet-Boudin, and P. Boulanger.** 1990. Human adenovirus-host cell interactions: comparative study with members of subgroups B and C. J. Virol. **64:**3661–3673.
11. **Huang, S., V. Reddy, N. Dasgupta, and G. R. Nemerow.** 1999. A single amino acid in the adenovirus type 37 fiber confers binding to human conjunctival cells. J. Virol. **73:**2798–2802.
12. **Mathias, P., M. Galleno, and G. R. Nemerow.** 1998. Interactions of soluble recombinant integrin alphav beta5 with human adenoviruses. J. Virol. **72:**8669–8675.
13. **Nemerow, G. R.** 2000. Adenovirus vectors—new insights. Trends Microbiol. **8:**391–393.
14. **Nemerow, G. R., and P. L. Stewart.** 1999. Role of αv integrins in adenovirus cell entry and gene delivery. Microbiol. Mol. Biol. Rev. **63:**725–734.
15. **Philipson, L., K. Lonberg-Holm, and U. Pettersson.** 1968. Virus-receptor interaction in an adenovirus system. J. Virol. **2:**1064–1075.
16. **Ritterband, D. C., and D. N. Friedberg.** 1998. Virus infections of the eye. Rev. Med. Virol. **8:**187–201.
17. **Roelvink, P. W., A. Lizonova, J. G. Lee, Y. Li, J. M. Bergelson, R. W. Finberg, D. E. Brough, I. Kovesdi, and T. J. Wickham.** 1998. The coxsackievirus-adenovirus receptor protein can function as a cellular attachment protein for adenovirus serotypes from subgroups A, C, D, E, and F. J. Virol. **72:**7909–7915.
18. **Schoehn, G., P. Fender, J. Chroboczek, and E. A. Hewat.** 1996. Adenovirus 3 penton dodecahedron exhibits structural changes of the base on fibre binding. EMBO J. **15:**6841–6846.
19. **Shah, A. K., and P. L. Stewart.** 1998. QVIEW: software for rapid selection of particles from digital electron micrographs. J. Struct. Biol. **123:**17–21.
20. **Shayakhmetov, D. M., and A. Lieber.** 2000. Dependence of adenovirus infectivity on length of the fiber shaft domain. J. Virol. **74:**10274–10286.
21. **Stevenson, S. C., M. Rollence, J. Marshall-Neff, and A. McClelland.** 1997. Selective targeting of human cells by a chimeric adenovirus vector containing a modified fiber protein. J. Virol. **71:**4782–4790.
22. **Stewart, P. L., R. M. Burnett, M. Cyrklaff, and S. D. Fuller.** 1991. Image reconstruction reveals the complex molecular organization of adenovirus. Cell **67:**145–154.
23. **Stewart, P. L., R. B. Cary, S. R. Peterson, and C. Y. Chiu.** 2000. Digitally collected cryo-electron micrographs for single particle reconstruction. Microsc. Res. Technol. **49:**224–232.
24. **Stewart, P. L., C. Y. Chiu, S. Huang, T. Muir, Y. Zhao, B. Chait, P. Mathias, and G. R. Nemerow.** 1997. Cryo-EM visualization of an exposed RGD epitope on adenovirus that escapes antibody neutralization. EMBO J. **16:**1189–1198.
25. **Stewart, P. L., S. D. Fuller, and R. M. Burnett.** 1993. Difference imaging of adenovirus: bridging the resolution gap between X-ray crystallography and electron microscopy. EMBO J. **12:**2589–2599.
26. **Tomko, R. P., R. Xu, and L. Philipson.** 1997. HCAR and MCAR: the human and mouse cellular receptors for subgroup C adenoviruses and group B coxsackieviruses. Proc. Natl. Acad. Sci. USA **94:**3352–3356.
27. **van Heel, M., G. Harauz, E. V. Orlova, R. Schmidt, and M. Schatz.** 1996. A new generation of the IMAGIC image processing system. J. Struct. Biol. **116:**17–24.
28. **van Raaij, J. M., N. Louis, J. Chroboczek, and S. Cusack.** 1999. Structure of the human adenovirus serotype 2 fiber head domain at 1.5 Å resolution. Virology **262:**333–343.
29. **van Raaij, J. M., A. Mitraki, G. Lavigne, and S. Cusack.** 1999. A triple beta-spiral in the adenovirus fibre shaft reveals a new structural motif for a fibrous protein. Nature **401:**935–938.
30. **Von Seggern, D. J., C. Y. Chiu, S. K. Fleck, P. L. Stewart, and G. R. Nemerow.** 1999. A helper-independent adenovirus vector with E1, E3, and fiber deleted: structure and infectivity of fiberless particles. J. Virol. **73:**1601–1608.
31. **Von Seggern, D. J., S. Huang, S. K. Fleck, S. C. Stevenson, and G. R. Nemerow.** 2000. Adenovirus vector pseudotyping in fiber-expressing cell lines: improved transduction of Epstein-Barr virus-transformed B cells. J. Virol. **74:**354–362.
32. **Wickham, T. J., P. Mathias, D. A. Cheresh, and G. R. Nemerow.** 1993. Integrins αvβ3 and αvβ5 promote adenovirus internalization but not virus attachment. Cell **73:**309–319.
33. **Wu, E., J. Fernandez, S. K. Fleck, D. J. Von Seggern, S. Huang, and G. R. Nemerow.** 2001. A 50 kDa membrane protein mediates sialic acid-independent binding and infection of conjunctival cells by adenovirus type 37. Virology **279:**78–89.
34. **Xia, D., L. J. Henry, R. D. Gerard, and J. Deisenhofer.** 1994. Crystal structure of the receptor-binding domain of adenovirus type 5 fiber protein at 1.7 Å resolution. Structure **2:**1259–1270.